GSA Data Repository 2019225

Gold, arsenic, and copper zoning in pyrite: a record of fluid chemistry and growth kinetics

Ya-Fei Wu[1,2], Denis Fougerouse [2,3], Katy Evans [2], Steven M. Reddy [2,3], David W. Saxey [3], Paul Guagliardo [4], Jian-Wei Li [1†]

[1] *State Key Laboratory of Geological Processes and Mineral Resources and School of Earth Resources, China University of Geosciences, Wuhan, Hubei Province 430074, China*

[2] *School of Earth and Planetary Sciences, Curtin University, GPO Box U1987, Perth, WA 6845, Australia*

[3] *Geoscience Atom Probe, Advanced Resource Characterisation Facility, John de Laeter Centre, Curtin University, GPO Box U1987, Perth, WA, 6845, Australia*

[4] *Centre for Microscopy, Characterisation and Analysis, The University of Western Australia, 35 Stirling Highway, Crawley, WA 6009, Australia*

A1. List of supplementary figures and tables

Figure DR1. Zoned (A), framboidal (B), and colloform (C) pyrite in the hydrothermal cements of Daqiao breccia ores. Py–Pyrite. Scale bar is 10 μm.

Figure DR2. Atom probe mass spectrum. Peaks are color-coded by atomic or molecular species.

Figure DR3. Line profile (B) and diagrams of mean elemental counts (C-E) for different regions on NanoSIMS arsenic ($^{75}As^{32}S$) map (A) showing the correlations between Cu, As, and Au.

Table DR1. Analysis and reconstruction parameters for atom probe data following recommendation of Blum et al. (2018).

Table DR2. Arsenic, Au, and Cu compositions of three atom probe specimens from the Daqiao Au-rich zoned pyrite.

A2. Analytical methods

A2.1 NanoSIMS analysis

NanoSIMS analysis was performed on polished epoxy mounts at the Centre for Microscopy, Characterisation and Analysis (CMCA) at the University of Western Australia (UWA), using a CAMECA NanoSIMS 50L optimized as described by Wu et al. (2019). A Cs^+ ion source with a spot size of approximately 50 nm was employed. Multiple electron multipliers record ion counts from the same sputtered sample volume at seven masses simultaneously.

Each region of interest was pre-sputtered using a beam current of 250 pA, to remove surface contaminants and implant Cs^+ ions into the sample matrix to achieve a steady state of secondary ion emission. Negative secondary ions of interest ($^{63}Cu^{32}S^-$, $^{75}As^{32}S^{--}$, and $^{197}Au^-$) were then sputtered from the sample surface using a beam current of ~2.5 pA. The electron gun was used for charge compensation because the samples were predominantly composed of insulating

materials. Analysis areas ranged in size from 15×15 to 40×40 μm^2, the image sizes were 256×256 to 512×512 pixels, and the dwell times were 40–160 ms per pixel. NanoSIMS images were processed using ImageJ. The ion intensity of each trace element provides a simple, semi-quantitative expression of localized trace element enrichment.

A2.2 Atom probe analysis

Three atom probe needle-shaped specimens (inset of Fig. 2A) from the zoned pyrite were prepared and analyzed at the Advanced Resource Characterization Facility at Curtin University. The specimens were prepared using a Tescan Lyra3 Focused Ion Beam Scanning Electron Microscope (FIB-SEM) with a Ga^+ ion source, employing standard lift-out techniques (Thompson et al., 2007). A Cameca LEAP 4000X HR in laser assisted mode was employed for analysis. Approximately 10 to 76 million ions (Table DR1) were collected from each specimen at an evaporation rate of 0.01 ions/pulse, a UV laser (λ = 355 nm) pulse energy of 30 to 50 pJ, and a pulse rate of 125 kHz, at a base temperature of 50 K. Peaks were identified and ranged using the Cameca IVAS 3.8 processing software (Fig. DR2). Compositions of specific domains were isolated by volumes defined by concentration isosurfaces (Hellman et al., 2000). The background noise, mass peak overlaps and detector saturation are assessed from the data sets themselves, with uncertainties typically comparable to those arising from the counting statistics for each atomic species. Minor overlapping of Au^+ by $FeAsS_2^+$ (e.g., $^{56}Fe^{75}As^{32}S^{34}S^+$) in specimen 3 (Fig. DR2) has been corrected via the percentage calculation and deduction of this part of $FeAsS_2^+$ molecule following the peak decomposition method (Sha et al., 1992; Dmitrieva et al., 2011). This overlap was significantly reduced by lowering the laser energy from 50 to 30 pJ. APT offers a novel method that allows atom-resolution quantitative three-dimensional

elemental mapping of ion distributions down to 10 appm (atomic parts per million) concentrations (Kelly and Larson, 2012).

A3. References cited

Blum, T.B., Darling, J.R., Kelly, T.F., Larson, D.J., Moser, D.E., Perez-Huerta, A., Prosa, T.J., Reddy, S.M., Reinhard, D.A., and Saxey, D.W., 2018, Best practices for reporting atom probe analysis of geological materials: Microstructural Geochronology: Planetary Records Down to Atom Scale, v. 232, p. 369–373.

Dmitrieva, O., Choi, P., Gerstl, S., Ponge, D., and Raabe, D., 2011, Pulsed-laser atom probe studies of a precipitation hardened maraging TRIP steel: Ultramicroscopy, v. 111, p. 623–627.

Hellman, O.C., Vandenbroucke, J.A., Rüsing, J., Isheim, D., and Seidman, D.N., 2000, Analysis of three-dimensional atom-probe data by the proximity histogram: Microscopy and Microanalysis, v. 6, p. 437–444.

Kelly, T.F., and Larson, D.J., 2012, Atom probe tomography 2012: Annual Review of Materials Research, v. 42, p. 1–31.

Sha, W., Chang, L., Smith, G., Cheng, L., and Mittemeijer, E., 1992, Some aspects of atom-probe analysis of Fe-C and Fe-N systems: Surface Science, v. 266, p. 416–423.

Thompson, K., Lawrence, D., Larson, D., Olson, J., Kelly, T., and Gorman, B., 2007, In situ site-specific specimen preparation for atom probe tomography: Ultramicroscopy, v. 107, p. 131–139.

Wu, Y.F., Evans, K., Li, J.W., Fougerouse, D., Large, R.R., and Guagliardo, P., 2019, Metal remobilization and ore-fluid perturbation during episodic replacement of auriferous pyrite

from an epizonal orogenic gold deposit: Geochimica et Cosmochimica Acta, v. 245, p. 98–117.

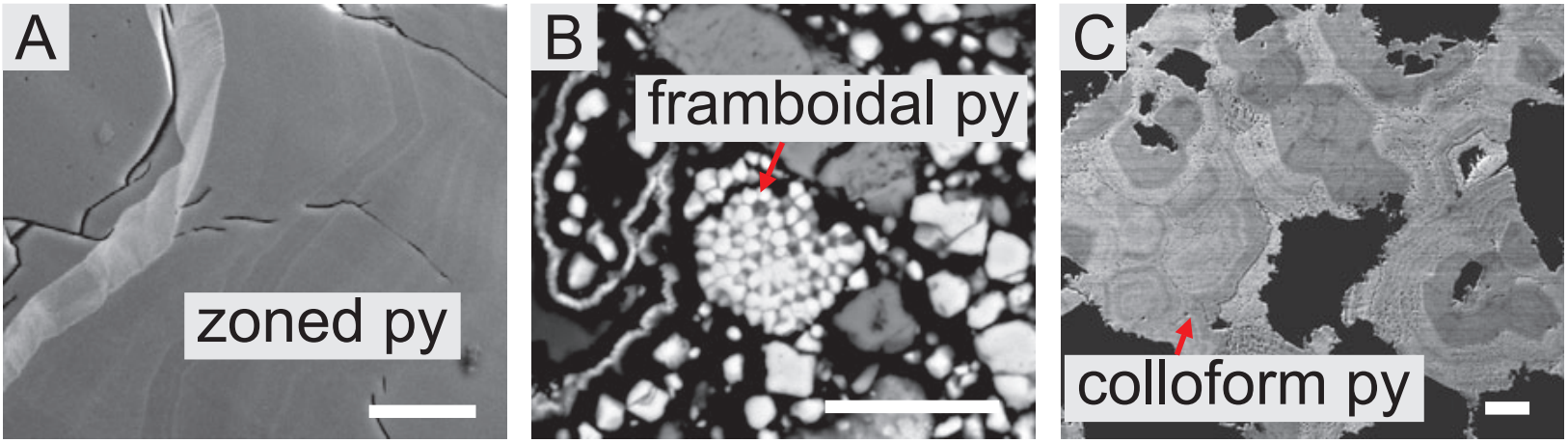

Fig. DR1

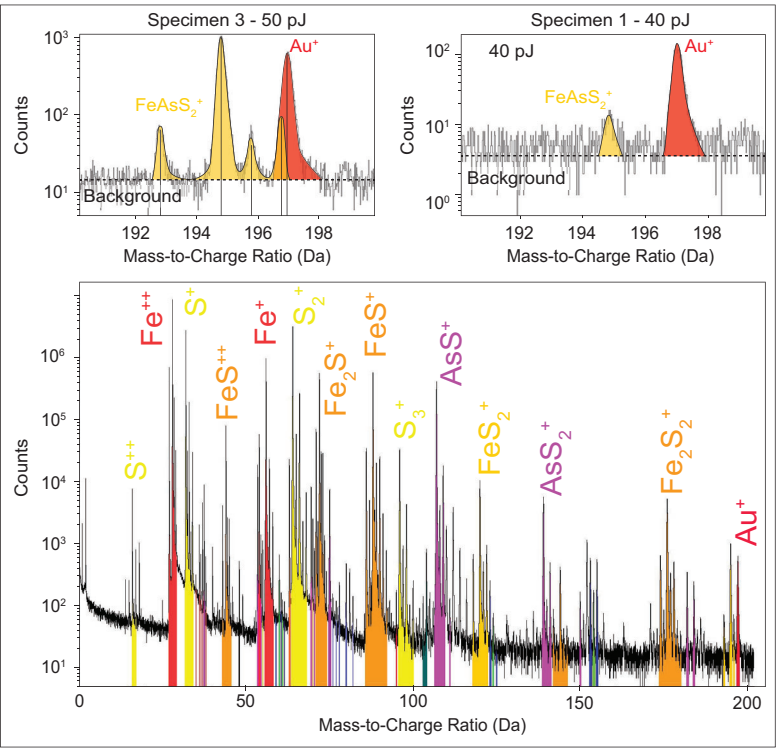
Specimen 3 - 50 pJ
Specimen 1 - 40 pJ
40 pJ
Au+
FeAsS2+
Background
Counts
Mass-to-Charge Ratio (Da)
Fe++
S+
FeS++
Fe+
S2+
Fe2S+
FeS+
S3+
AsS+
FeS2+
AsS2+
Fe2S2+
S++
Au+

Fig. DR2

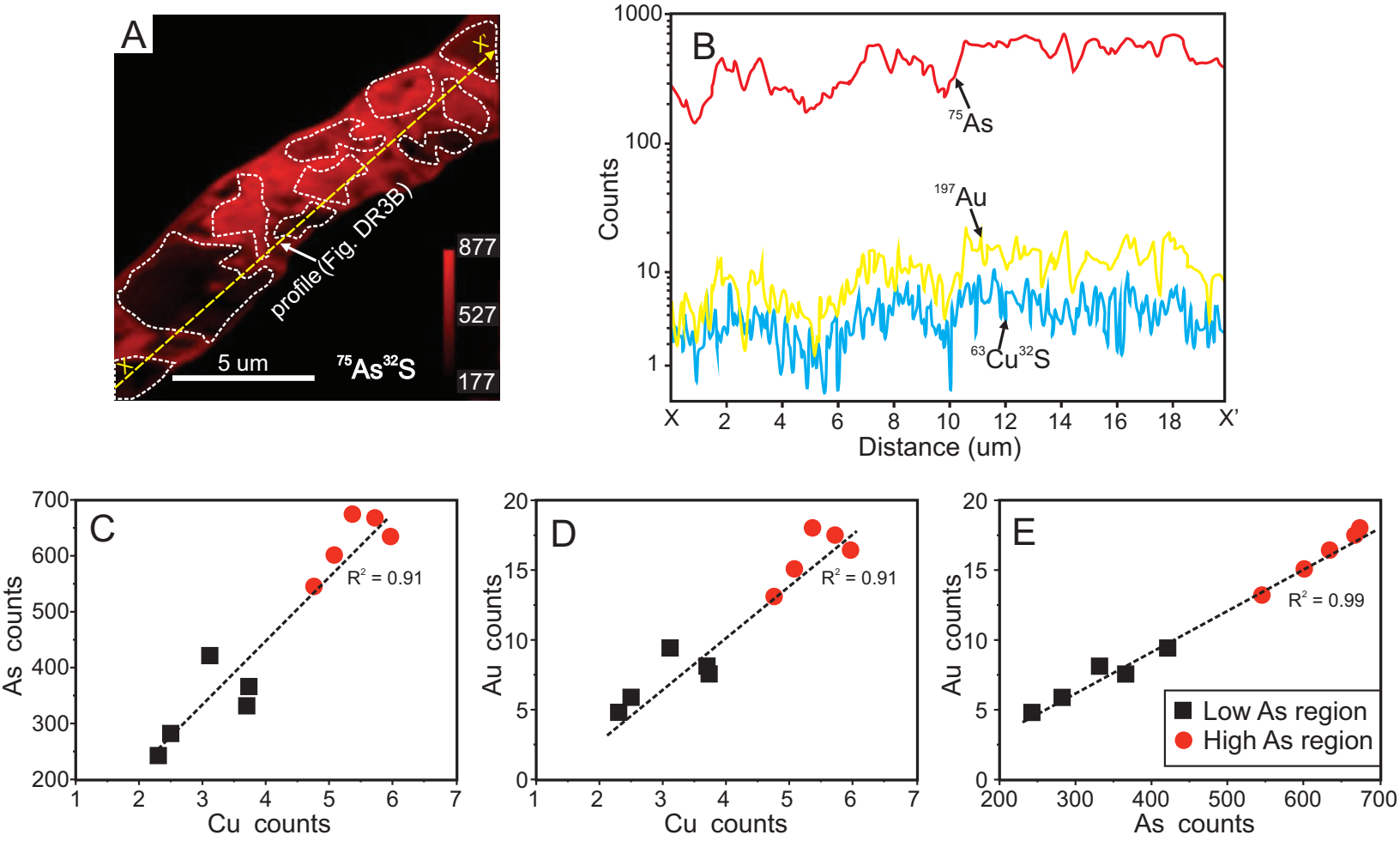
A
profile (Fig. DR3B)
877
527
177
5 um
75As32S
B
Counts
75As
197Au
63Cu32S
Distance (um)
X
X'
C
As counts
Cu counts
R2 = 0.91
D
Au counts
Cu counts
R2 = 0.91
E
Au counts
As counts
R2 = 0.99
Low As region
High As region

Fig. DR3

TABLE DR1. ANALYSIS AND RECONSTRUCTION PARAMETERS FOR ATOM PROBE DATA FOLLOWING RECOMMENDATION OF BLUM ET AL. (2018).

Specimen/data Set	Specimen 1	Specimen 2	Specimen 3
Instrument model		LEAP 4000X HR	
Instrument settings			
Laser wavelength (nm)	355	355	355
Laser pulse energy (pJ)	30	40	50
Pulse frequency (kHz)	125	125	125
Evaporation control	Detection rate	Detection rate	Detection rate
Target detection rate (ions/pulse)	0.01	0.01	0.01
Nominal flight path (mm)	382	382	382
Set point temperature (K)	50	50	50
Chamber pressure (Torr)	1.3×10^{-10}	1.3×10^{-10}	1.2×10^{-10}
Data summary			
LAS root version	15.41.342l	15.41.342l	15.41.342l
CAMECAROOT version	18.44.416	18.44.416	18.44.416
Analysis software	IVAS 3.8	IVAS 3.8	IVAS 3.8
Total ions:	12,417,315	10,490,929	76,251,106
Single	56.4%	60.2%	62.6%
Multiple	42.6%	38.8%	36.7%
Partial	1.1%	1.0%	0.7%
Reconstructed ions:	11,813,609	9,216,276	72,600,477
Ranged	98.3%	98.9%	99.1%
Unranged	1.7%	1.1%	0.9%
Volt./bowl corr. peak (Da)	16	16	16
Mass calib. (peaks/interp.)	5/Lin.	4/Lin.	5/Lin.
$^{\dagger}(M/\Delta M)$ for $^{32}S^{++}$	666.6	707.1	822.8
$^{\dagger\dagger}(M/\Delta M_{10})$	296.6	333.3	405.4
time independent background (ppm/ns)	2.5	2.1	1.8
Reconstruction			
Final specimen state	Fractured	Fractured	Fractured
Pre-/post-analysis imaging	SEM/n.a.	SEM/n.a.	SEM/n.a.
Radius evolution model	“voltage”	“voltage”	“voltage”
Field factor (k)	3.3	3.3	3.3
Image compression factor	1.65	1.65	1.65
Assumed e-field (V/nm)	33	33	33
Detector efficiency	36%	36%	36%
Avg. atomic volume (nm^3)	0.0108	0.0108	0.0108
$V_{initial}$ (V)	2,474	3,566	3,048

$^{\dagger}\Delta M$ is full width at half maximum.

$^{\dagger\dagger}\Delta M_{10}$ is full width at tenth maximum.

TABLE DR2. ARSENIC, Au, AND Cu COMPOSITIONS OF THREE ATOM PROBE SPECIMENS FROM THE DAQIAO Au-RICH ZONED PYRITE.

Specimen no.	Arsenic (As) regions	As (at. %)	Au (appm)	Cu (appm)
Specimen 1	Homogeneous As	4.30 ± 0.01	131 ± 3	1028 ± 8
Specimen 2	High-As region	4.28 ± 0.01	164 ± 5	1189 ± 14
	Low-As region	2.11 ± 0.01	71 ± 3	640 ± 10
Specimen 3	High-As region	4.35 ± 0.01	118 ± 6	1087 ± 17
	Low-As region	2.22 ± 0.01	54 ± 4	713 ± 14
Mean		3.45 ± 1.05	108 ± 40	931 ± 216